J. Fluid Mech. (1994), *vol.* 269, *pp.* 23–44

The transient behaviour of alloys solidified from below prior to the formation of chimneys

By M. GRAE WORSTER[1] AND ROSS C. KERR[2]

[1] Institute of Theoretical Geophysics, Department of Applied Mathematics and Theoretical Physics, University of Cambridge, Silver Street, Cambridge CB3 9EW, UK

[2] Research School of Earth Sciences, Australian National University, GPO Box 4, Canberra 2601, ACT, Australia

(Received 4 June 1993 and in revised form 2 November 1993)

We investigate interactions between interfacial disequilibrium and compositional convection during the freezing of an alloy from below to form a mushy layer. A theoretical model is developed in which a stagnant mushy layer underlies a melt that is convecting vigorously, driven by compositional gradients associated with undercooling at the mush–liquid interface. In a series of laboratory experiments, we measure the interfacial undercooling in aqueous solutions of ammonium chloride contaminated to varying degrees by copper sulphate. It has recently been found (Huppert & Hallworth 1993) that a small amount of copper sulphate added to a solution of ammonium chloride significantly inhibits the formation of chimneys in the mushy layer that forms when the solution is cooled below its liquidus. It is our thesis that this phenomenon can be explained in large part by the consequences of the interactions between compositional convection and interfacial undercooling that are investigated herein. The measured undercooling is a function of the rate of advance of the interface and is found to be a very strong, increasing function of the concentration of copper sulphate in solution. The theoretical model is evaluated using parameter values appropriate to the experimental system and it is found that the transient development of the mushy layer depends significantly on the level of interfacial disequilibrium. In particular, it is predicted that the time taken for the Rayleigh number associated with the mushy layer to reach any particular value increases enormously as the level of interfacial disequilibrium increases and that the Rayleigh number can have an upper bound that is less than the critical value needed for the onset of convection within the mushy layer. This suggests that the formation of chimneys in the mushy layer can be similarly delayed or prohibited, in agreement with the experimental findings of Huppert & Hallworth (1993). Additionally, the model predicts that under certain conditions the solid fraction can increase away from the cooled boundary leading to trapping of the interstitial liquid. The model also describes a mechanism for macrosegregation of alloys cooled and solidified from below.

1. Introduction

Buoyancy-driven convection can have a significant influence on the composition and structure of metal castings. However, in traditional metallurgical research such convection could only be inferred *post mortem* from etchings of quenched, partially solidified ingots. In 1970, Copley *et al.* suggested using a transparent analogue system, namely an aqueous solution of ammonium chloride (NH_4Cl), in order to observe the convection directly. They chose this particular salt on the grounds that, in common

with most metals, it has a low entropy of fusion and forms highly branched, rather than prism-like, crystals. Their major observation was the formation of 'chimneys' in the mushy layer. These are narrow vertical channels, devoid of crystals, which they proposed were a cause of freckling in castings. It was clear from these experiments that chimneys are associated with convection of the melt in the interstices of the mushy layer, since a buoyant plume of residual melt emanated from each chimney. Since the experiments of Copley *et al.* (1970), aqueous solutions of ammonium chloride have been the most common transparent systems to be used in experimental investigations of convection during the solidification of alloys. Consequently, their behaviour has had a profound influence on the development of ideas and theories about how alloys solidify.

However, as has been noted by Huppert (1990), a number of other aqueous salt solutions behave quite differently from ammonium chloride. In particular, chimneys have rarely been seen in experiments using solutions of salts other than ammonium chloride. Although ammonium chloride appears to fulfil its role as an analogue for metallic systems, the importance of solidification extends beyond the realms of metallurgy (to organic chemistry and geology, for example), and it is necessary to understand the underlying causes of such differences and to be able to determine quantitatively when certain behaviours are to be expected. A number of researchers have informally noted the differences between ammonium chloride and the other salts (for example, ammonium chloride has a much lower entropy of fusion and forms unhydrated, dendritic crystals, while the others typically form hydrated and faceted crystals) without explaining how or why these differences affect the propensity to form chimneys.

A recent series of experiments (Huppert & Hallworth 1993) may allow a systematic study of these questions. These investigators added small amounts of copper sulphate ($CuSO_4$) (up to 1 wt%) to solutions of ammonium chloride (27 wt%) in water. Their principal observation was that, as the level of contamination by $CuSO_4$ increased, the time taken for chimneys to appear in the system increased until, at about 0.5 wt% $CuSO_4$, no chimneys were observed at all. They also noted that the nature of the crystals in the mushy layer changed, becoming more faceted as the level of contamination increased. In an appendix to Huppert & Hallworth (1993), S. Lipson suggested that, in the more faceted systems, the interstitial fluid might be supersaturated and might therefore be able to rise convectively out of the mushy layer before causing any dissolution of the crystals. This is a qualitative explanation for why chimneys may not form even once the interstitial fluid is convecting. In this paper, we provide a different, quantitative assessment of Huppert & Hallworth's results. We show how the contamination can cause a delay in the onset of convection within the mushy layer and may suppress such convection entirely within any particular experiment.

Essential to our explanation is the coupling between convection and disequilibrium (undercooling) at the mush–liquid interface. This paper draws together ideas about the nature of compositional convection in and above mushy layers (Worster 1992) and about the coupling between interfacial undercooling and turbulent convection in the melt (Kerr *et al.* 1990*b*).

Worster (1992) conducted a linear-stability analysis of the onset of compositional convection in an alloy being solidified from below. He showed that convection can be initiated both from within the mushy layer and from within a compositional boundary layer situated in the melt above and adjacent to the mush–liquid interface. These two modes of convection (the mushy-layer mode and the boundary-layer mode) have distinct characteristics. The boundary-layer mode has a wavelength comparable to the

compositional-diffusion length and a flow that barely penetrates the mushy layer. The mushy-layer mode, by contrast, has a much larger wavelength, comparable to the depth of the mushy layer, and causes dissolution of the solid in regions of upflow. Worster (1992) conjectured that it is the mushy-layer mode that is primarily responsible for the formation of chimneys.

It has been found in many experiments (Chen & Chen 1991; Tait & Jaupart 1992) that small-scale convection in the melt above the mushy layer exists for some time before any convection is observed within the mushy layer and chimneys form. One must ask, therefore, how the small-scale convection might affect the onset of convection within the mushy layer. Emms & Fowler (1994) have recently analysed the stability of the mushy-layer mode of convection taking into account, in an averaged way, fully developed convection in the liquid above the mushy layer. Although the latter convection enhances somewhat the heat and mass fluxes from the liquid to the mushy region, Emms & Fowler found that this had little effect upon the onset of the mushy-layer mode. However, all these previous stability analyses have considered steady solidification in a semi-infinite domain and employed the approximations of equilibrium thermodynamics. In this paper, by contrast, we take account of convection in a finite domain, which causes the melt to evolve, and we incorporate the essential effects of disequilibrium at the mush–liquid interface.

The interface between the mushy layer and the melt is always undercooled, which is to say that the interfacial temperature is below the local liquidus temperature of the melt. The degree of undercooling is usually small and confined to the near neighbourhood of the interface. It can often be safely neglected, particularly when the only mechanism for heat and mass transport in the system is molecular diffusion. However, it has been found that such interfacial undercooling can have large, global consequences when coupled with thermal convection in the melt (Flood & Hunt 1987; Kerr *et al.* 1990*b*). Indeed, the interfacial undercooling itself can provide sufficient buoyancy to drive vigorous thermal convection in the melt (Worster, Huppert & Sparks 1990, 1993). Here, we examine the compositional convection of the melt that is driven by interfacial disequilibrium, while the mushy layer is assumed to remain stagnant. The consequent evolution of the melt and the mushy layer is determined and we assess how this affects the onset of convection within the mushy layer.

In §2, we describe the theoretical model and set out the equations governing the evolution of the melt and the mushy layer. Disequilibrium is accounted for by a simple kinetic growth law whose form is suggested by a series of experiments that we report in §3. These same experiments allow the determination of the value of the kinetic coefficient as it varies with the level of contamination by $CuSO_4$ in aqueous solutions of NH_4Cl. We use the measured kinetic growth law in a numerical evaluation of the theoretical model to show how the evolution of the system varies with the level of contamination while the mushy layer remains stagnant. These results, presented in §4, are used in §5 to interpret the experimental observation of Huppert & Hallworth (1993) regarding the delay in the formation of chimneys with increasing levels of contamination. The paper concludes in §6 with a discussion of other important consequences of the coupling between compositional convection and interfacial disequilibrium. In an addendum, §7, we briefly describe some similar experiments using aqueous solutions of ammonium bromide.

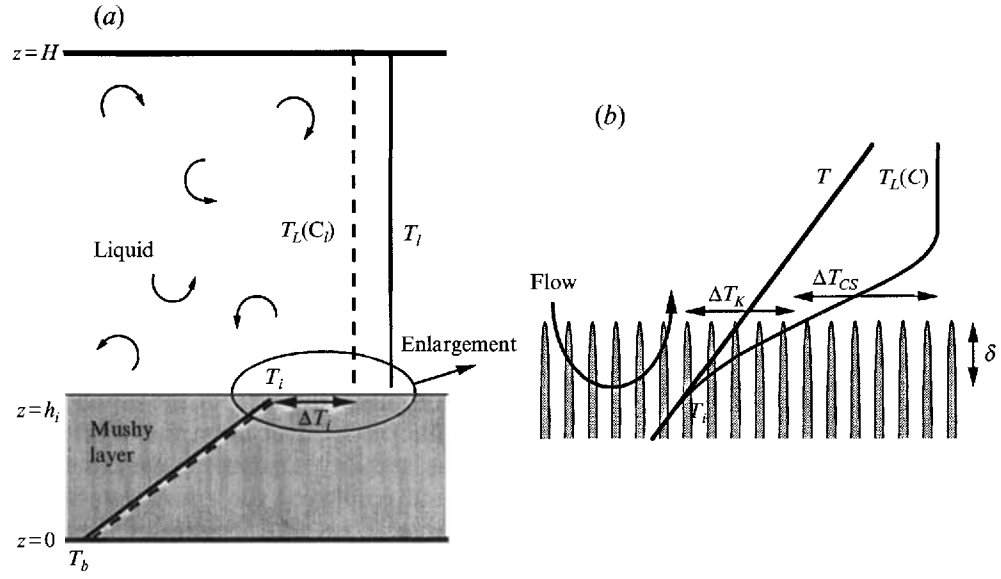

FIGURE 1. (*a*) A schematic diagram of the macroscopic view on which the theoretical model is based. A mushy layer grows upwards from the cooled base at $z = 0$. The temperature T is assumed to be equal to the local liquidus temperature $T_L(C)$ throughout the mushy layer. There are discontinuities between the values of the temperature and concentration in the mushy layer at the mush–liquid interface and their values T_l and C_l in the liquid, which vary with time but are assumed spatially uniform. (*b*) A conjectured view of the microscopic details of the mush–liquid interface. The convection in the liquid region penetrates a small distance δ below the interface. By assumption, this depth also marks the apparent interface (at temperature T_i) below which local thermodynamic equilibrium pertains. Above this level, there is a region of disequilibrium partly within the mushy layer (giving the undercooling ΔT_K) and partly within the liquid region (giving the undercooling ΔT_{CS}). In the experiments, only the gross undercooling $\Delta T_i = \Delta T_K + \Delta T_{CS}$, indicated in the macroscopic view, is measured.

2. The model

The system to be analysed is sketched in figure 1. A rectangular mould containing a binary melt of initial temperature T_0 and composition C_0 is cooled at its lower, horizontal boundary while all the other boundaries are insulated. The temperature T_b of the cooled base is taken to be less than the liquidus temperature $T_L(C_0)$ but greater than the eutectic temperature so that a mushy layer grows upwards from the boundary and no region is completely solid. The mushy layer fills the region $0 < z < h_i$, and the temperature of the mush–liquid interface is T_i. As illustrated in figure 1(*b*), which shows an enlargement of the interfacial region, we imagine that the interface is located slightly below the tips of the crystals that make up the mushy layer. This is explained in more detail later in this section.

The interstitial liquid in the mushy layer is assumed to be stagnant, while the region of melt above the mushy layer is assumed to be convecting vigorously. The convection is driven by the solutal buoyancy of the residual melt in the neighbourhood of the mush–liquid interface. There is evidence from a number of laboratory experiments (Tait & Jaupart 1989; Huppert 1990) that convection of the melt can occur throughout the solidification process without any apparent motion of the liquid in the mushy layer. This situation is also observed in the early stages of experiments using ammonium chloride before chimneys are formed (Chen & Chen 1991; Tait & Jaupart 1992). Often, as is the case for the experiments with ammonium chloride, the convection is rather

weak and takes the form of organized, double-diffusive fingers. In some other experiments, the convection is stronger and has the appearance of turbulent convective flow. These two possibilities are discussed further in §4.

The following model equations are similar to those described by Kerr *et al.* (1990*b*), who considered thermally driven convection of the melt in systems cooled from above. In their model there was no flux of solute. In contrast, we consider convection driven by solutal buoyancy, which enhances the transport of both heat and solute in the melt (Woods & Huppert 1989).

Within the mushy layer, the temperature field satisfies the nonlinear diffusion equation

$$c_m \frac{\partial T}{\partial t} = \frac{\partial}{\partial z}\left(k_m \frac{\partial T}{\partial z}\right), \tag{2.1}$$

where

$$k_m = k_\beta \phi + k_l(1-\phi) \tag{2.2}$$

and

$$c_m = c_\beta \phi + c_l(1-\phi) + \frac{\mathscr{L}_\beta C_L'(T)}{C_\beta - \bar{C}}(1-\phi)^2. \tag{2.3}$$

The solid fraction ϕ is given by

$$\phi = \frac{\bar{C} - C_L(T)}{C_\beta - C_L(T)}, \tag{2.4}$$

where C_β is the uniform composition of the solid phase of the mushy layer, $C_L(T)$ is the liquidus concentration at temperature T according to the equilibrium phase diagram, $C_L'(T)$ is the slope of the liquidus temperature, and $\bar{C}$ is the horizontally averaged bulk composition of the mushy layer. The physical parameters introduced above are the conductivity k, the specific heat capacity per unit volume c and the latent heat per unit volume of solid $\mathscr{L}$. Subscripts l, β and m denote properties of the liquid, the crystals within the mushy layer and the mean values for the mushy layer respectively.

The boundary conditions to be applied to (2.1) are

$$T = T_b \quad (z = 0) \tag{2.5a}$$

and

$$T = T_i \quad (z = h_i), \tag{2.5b}$$

in which the interfacial temperature T_i is an unknown to be determined.

The rate of advance of the mush–liquid interface is determined from a kinetic growth law

$$\dot{h}_i = \mathscr{G}(T_L(C_l) - T_i)^2, \tag{2.6}$$

where $T_L(C_l)$ is the liquidus temperature evaluated at the concentration C_l of the well-mixed melt, and $\mathscr{G}$ is the kinetic growth parameter. Kerr *et al.* (1990*b*) found a linear relationship between the growth rate $\dot{h}_i$ and the undercooling $T_L(C_l) - T_i$ for growth of ice crystals from a mixture of water and isopropanol. Here, we use the quadratic relationship (2.6), which has been found to give the best fit to data from experiments in which mushy layers are grown from aqueous solutions of ammonium chloride contaminated by small amounts of copper sulphate (see next section). A similar quadratic law is known to be appropriate for crystals growing by the mechanism of screw dislocations (Kirkpatrick, Robinson & Hayes 1976) and has been used by Worster *et al.* (1990, 1993) to model the growth of diopside crystals from a mixture of diopside and anorthite. A quadratic relationship between the undercooling and rate of advance of the interface between a slurry and a liquid region is also derived from thermodynamic principles by Hills & Roberts (1993) in the case when the undercooling is determined solely by the Gibbs–Thomson effect.

As shown in figure 1(*b*), the gross undercooling that we consider here is the sum of two contributions $\Delta T_i \equiv T_L(C_l) - T_i = \Delta T_{CS} + \Delta T_K$. We have assumed that the interior of the mushy layer is in local thermodynamic equilibrium. This assumption is likely to break down near the mush–liquid interface where the specific surface area of phase boundaries is relatively small. We therefore expect a narrow boundary layer within the mushy layer in which there is a significant departure from equilibrium, and T_i is taken to be the temperature just below this boundary layer. The undercooling ΔT_K between T_i and the temperature at the tips of the dendrites is a combination of the kinetic undercooling associated with molecular attachment rates and an undercooling associated with the curvature of the dendritic phase boundaries according to the Gibbs–Thompson relationship. Just ahead of the tips of the dendrites, there is a compositional boundary layer in the liquid, across which there is a difference ΔT_{CS} in the local liquidus temperature. This undercooling is that attributed to constitutional supercooling. These local details remain to be modelled or measured adequately. The undercooling that we measured experimentally (see next section) is the gross undercooling ΔT_i and we assume in addition that convection is driven by the total compositional difference $\Delta C_i = \Delta T_i / \Gamma = C_l - C_i$, where Γ is the slope of the liquidus, which is here assumed to be constant.

The interfacial temperature T_i is determined from the Stefan condition

$$\mathscr{L}_\beta \phi_i \dot{h}_i = k_m \left.\frac{\partial T}{\partial z}\right|_{h_i-} - c_l(T_l - T_i)\dot{h}_i - F_T, \tag{2.7}$$

which expresses conservation of heat at the interface. An explicit formula for the convective heat transfer F_T from the liquid to the mushy layer is given below. Conservation of solute across the mush–liquid interface requires that

$$(C_l - \bar{C})\dot{h}_i = -F_C, \tag{2.8}$$

where F_C is the rate of solute transfer from the liquid to the mushy layer.

The model is completed with equations determining the evolution of the melt caused by convective transfer of heat and solute across the mush–liquid interface. These can be expressed simply as

$$c_l(H - h_i)\dot{T}_l = -F_T \tag{2.9}$$

and

$$(H - h_i)\dot{C}_l = -F_C. \tag{2.10}$$

The convective flux of solute F_C is driven by the compositional difference $C_l - C_i$ between the liquid region and the mush–liquid interface, where $C_i = C_L(T_i)$ is the composition of the liquid phase of the mushy layer at the interface. A scaling analysis based on the assumption that the convective flux should be independent of the depth of the liquid region when the Rayleigh number is large leads to the familiar 'four-thirds law',

$$F_C = 2^{\frac{4}{3}} \lambda D \left(\frac{\beta g}{D\nu}\right)^{\frac{1}{3}} (C_l - C_i)^{\frac{4}{3}}, \tag{2.11}$$

where the parameter λ may depend upon the buoyancy ratio $\alpha \Delta T_l / \beta \Delta C_i$, $\Delta T_l = T_l - T_i$ is the temperature difference between the interface and the melt, and α is the thermal expansion coefficient (Turner 1979). The other physical parameters on which this relationship depend are the solutal diffusion coefficient D, the solutal expansion coefficient β, the kinematic viscosity of the liquid ν and the acceleration due to gravity g. Dimensional analysis can also be used to show that the thermal flux is given by an expression of the form

$$F_T = A c_l \left(\frac{T_l - T_i}{C_l - C_i}\right) F_C, \tag{2.12}$$

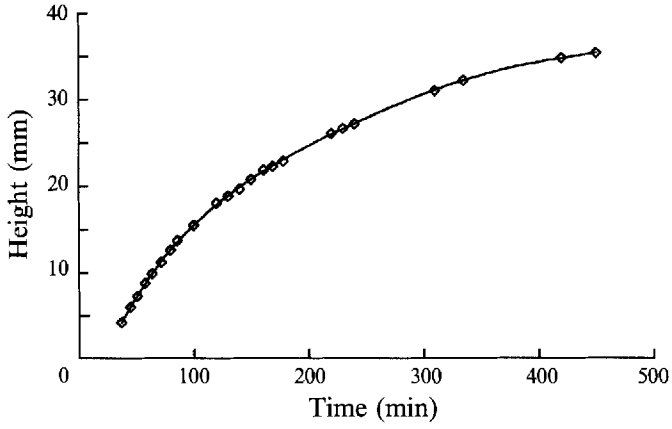

FIGURE 2. Data of the measured depth of the mushy layer as a function of time in a typical experiment. The solid curve is the best-fit fifth-order polynomial used to determine the growth rate of the mushy layer.

where A is a constant that depends upon the ratio of thermal to solutal diffusivities (Huppert 1990). Woods & Huppert (1989) derived more explicit expressions of the form (2.12) for three particular pictures of how the thermal and compositional boundary layers interact. These will be described briefly in §4.

3. Experimental determination of interfacial undercooling

A central feature of the proposed model is the undercooling at the mush–liquid interface. It is the degree of undercooling that we believe is one of the key parameters governing the transient behaviour of solidifying melts that are simultaneously convecting. In particular, we aim to show that changes in the undercooling parameter $\mathscr{G}$ are primarily responsible for the delay in the appearance of chimneys when solutions of ammonium chloride solidified from below are contaminated with copper sulphate (Huppert & Hallworth 1993). We therefore conducted a series of experiments designed to measure the degree of undercooling at the mush–liquid interface as it varies with the rate of advance at the interface and the level of contamination.

A Perspex tank with a stainless steel base, 12.5 × 12.6 cm in horizontal cross-section was filled to a depth of 37.5 cm with a saturated solution of ammonium chloride in water. For example, when the room temperature was 20 °C, the concentration of the solution was about 27 wt% NH_4Cl. To this solution was added a small quantity of copper sulphate, the precise amount varying from experiment to experiment. The temperature of the base of the tank was maintained at an approximately constant value lower than the initial liquidus temperature of the solution. A mushy layer of ammonium-chloride dendrites grew upwards from the cooled base. No measurements were taken after chimneys had begun to form in the mushy layer.

As the experiment evolved, we measured the position of the mush–liquid interface at frequent time intervals. A low-order polynomial gave a good fit to these data (figure 2), and this polynomial was differentiated to determine the rate of advance of the interface as a function of time. In addition, we noted the times at which the interface passed a number of fixed thermistors, recording at those times the temperature of the interface and the concentration of the liquid a few millimetres above the interface. The rate of advance of the interface at those times is plotted against the measured interfacial undercooling in figure 3(*a*).

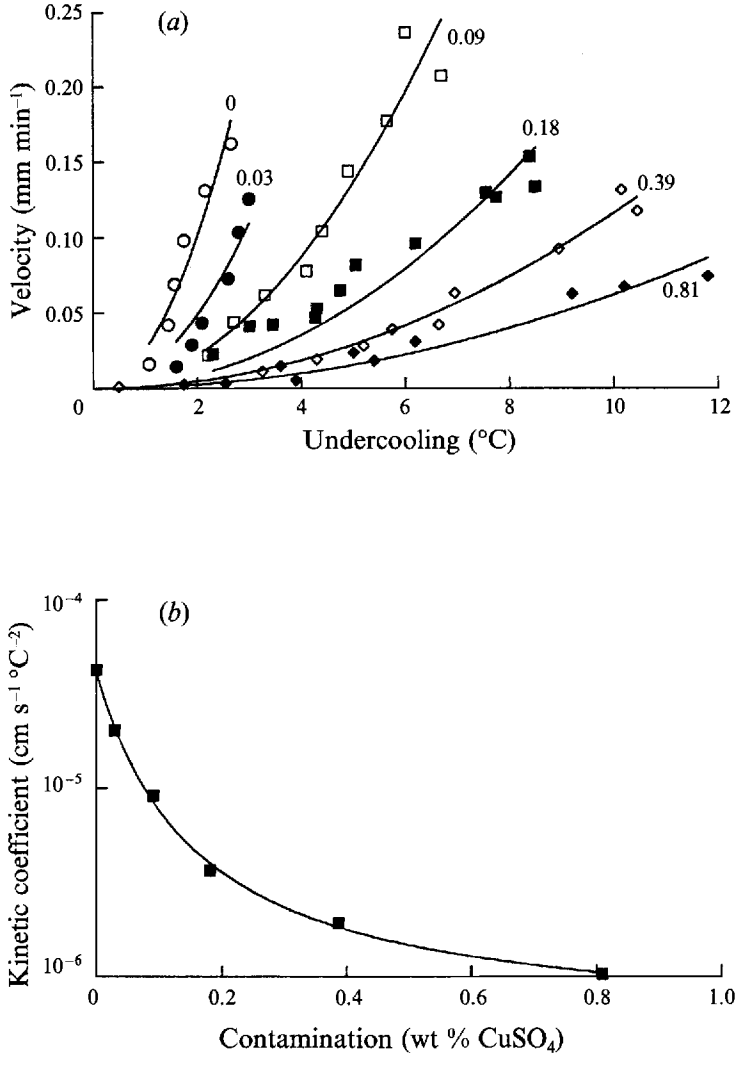

FIGURE 3. (*a*) Experimental data of the rate of advance of the mush–liquid interface plotted against the interfacial undercooling. The results of several different experiments are shown. Results from experiments that used the same level of contamination (indicated in wt % $CuSO_4$ by the numbers on the graph) are plotted using the same symbol. The solid curves represent the best-fit second-order power law for each set of data for the same level of contamination. (*b*) The coefficients of the power laws found from (*a*) plotted as a function of the level of contamination. The solid curve is the smooth interpolating function given by (3.1).

It is immediately apparent from figure 3(*a*) that the rate of advance of the mush–liquid interface varies with interfacial undercooling and that it decreases, for a given undercooling, as the level of contamination increases. Alternatively, figure 3(*a*) can be read as showing much greater departures from equilibrium (undercooling), for a given growth rate, in the more contaminated systems. In order to quantify these effects in a convenient way for inclusion in the theoretical model, it was decided to fit the data of figure 3(*a*) using a simple power law. The best overall fit to the suite of data was given by quadratic relationships of the form (2.6), as shown by the solid curves in figure 3(*a*). The kinetic coefficient $\mathscr{G}$ associated with each curve is plotted in figure 3(*b*),

which shows the kinetic coefficient as a function of contamination. These data are fitted by the function

$$\mathscr{G} = 4.14 \times 10^{-5} \exp\left[\frac{-27.4\xi}{1+6.21\xi}\right] \text{cm s}^{-1} \,^{\circ}\text{C}^{-2}, \tag{3.1}$$

where ξ is the weight percent contamination by $CuSO_4$. This function conveniently interpolates the data, as shown in figure 3(*b*). Its form has no theoretical basis and it should not be used to extrapolate the data for higher values of the contamination.

Note that the kinetic coefficient changes very rapidly with contamination; it changes by a factor of 10 for a contamination of a pure NH_4Cl solution by less than 0.2 wt% $CuSO_4$. Such large changes are much greater than any experimental error, so we are confident in using (2.6) and (3.1) to determine the gross behaviour of these crystallizing systems.

4. Calculations

The model described in §2 was evaluated using physical parameter values relevant to the NH_4Cl–$CuSO_4$–H_2O system (table 1), and values for the kinetic coefficient were evaluated using (3.1). Appropriate values for the coefficients λ and A need to be chosen.

Woods & Huppert (1989) considered three different pictures of how the compositional convection interacts with the stable thermal gradient to determine how the flux ratio A depends on the ratio of diffusivities D/κ. Their discussion can be summarized briefly as follows. If compositional convective plumes rise through the thermal boundary layer without significantly disturbing it then $A = O(1)$ when $D/\kappa \ll 1$. This would be the case for rather weak compositional buoyancy relative to the stable thermal buoyancy. If the buoyancy ratio is larger and the compositional convection is more vigorous then A can be $O((\kappa/D)^{\frac{1}{2}})$ or $O(\kappa/D)$ depending on whether the thermal boundary layer can grow diffusively between convective bursts of the compositional boundary layer or whether the compositional convection can keep the entire region of fluid above the compositional boundary layer well mixed.

In the experiments with NH_4Cl–H_2O, the convection is quite weak and usually takes the form of double-diffusive fingers. We expect therefore that A should be about unity. However, as shown in figure 4, the value of A has little effect on the rate of growth of the mushy layer, which is determined primarily by the balance between the release of latent heat and conduction back through the layer (Turner, Huppert & Sparks 1986; Kerr *et al.* 1990*a*). The principal effect of varying A is to alter the rate of cooling of the liquid region, which we shall not be concerned with here, and causes the crossings of the curves in figure 4. The details of the temperature evolution, including such crossings, are discussed at length by Kerr *et al.* (1990*a*). In what follows, we choose the value $A = 1$.

The coefficient λ is about 0.1 for single-component convection from a horizontal flat plate (Howard 1966; Turner 1979). It should be a little smaller than this when there is a second component (here temperature) having a stabilizing influence on the density field. However, it might be expected that λ is larger for convection from a mush–liquid interface, where the exposed surface area of the dendrite tips is larger than the horizontal area (figure 1*b*). The primary effect of increasing λ is to enhance the rate at which solute is brought into the mushy layer and deposited to increase the solid fraction. Thus there is a greater release of latent heat, which retards growth of the mushy layer. This is illustrated in figure 5(*a*, *b*), where calculations for the depth of the

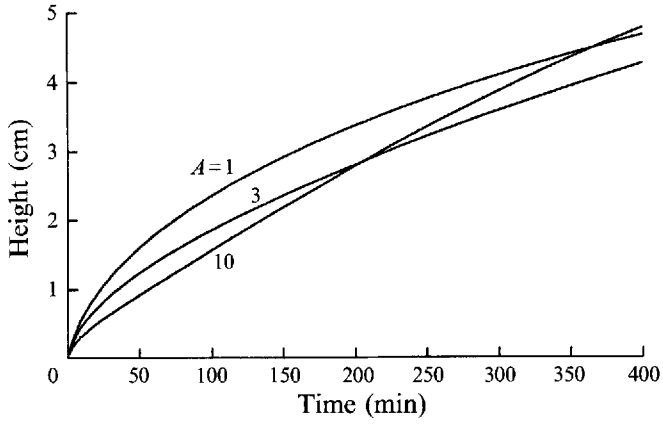

FIGURE 4. Predictions of the height of the mushy layer as a function of time for three different values of the flux ratio A. The details of these curves are similar to those described in detail by Kerr *et al.* (1990*a*).

Quantity	Symbol	Value	Units
Specific heat of crystal per unit volume	c_β	0.545	cal cm^{-3} $°C^{-1}$
Specific heat of solution per unit volume	c_l	0.847	cal cm^{-3} $°C^{-1}$
Thermal conductivity of crystal	k_β	5.26×10^{-3}	cal cm^{-1} s^{-1} $°C^{-1}$
Thermal conductivity of solution	k_l	1.39×10^{-3}	cal cm^{-1} s^{-1} $°C^{-1}$
Heat of solution per unit volume	$\mathscr{L}_\beta$	100.8	cal cm^{-3}
Solute diffusion coefficient	D	10^{-5}	cm^2 s^{-1}
Solutal expansion coefficient	β	2.5×10^{-3}	wt $\%^{-1}$
Kinematic viscosity of solution	ν	0.93×10^{-2}	cm^2 s^{-1}
Initial depth of solution	H	36	cm
Initial temperature of solution	T_0	20	°C
Initial concentration of solution	C_0	27	wt % NH_4Cl
Temperature of cooled base	T_b	−15.9	°C
Liquidus temperature	$T_L(C)$	$-15.9+4.79(C-19.7)$	°C
Liquidus concentration	$C_L(T)$	$19.7+0.209(T+15.9)$	wt %
Liquidus slope	Γ	4.79	°C wt $\%^{-1}$

TABLE 1. The parameter values used in calculations.

mushy layer and the mean solid fraction within the mushy layer are presented as functions of time for a few values of λ. The parameter values used are those in table 1, with the kinetic coefficient $\mathscr{G}$ given by (3.1) when $\xi = 0.5$. On the same graphs is plotted data of Huppert & Hallworth (1993) from one of their experiments with a contamination of 0.5 wt% $CuSO_4$, in which chimneys were never observed. We see that it is not possible to choose a value of λ that allows a fit to both sets of data simultaneously. We attribute this partly to the neglect of contraction in the mathematical model (i.e. to the assumption that solid and liquid have equal densities), which, if included, would cause the predictions of both height and solid fraction to decrease by approximately 20% in this case (Chiareli, Huppert & Worster 1994). Given this, the appropriate value of λ is probably in the region of 0.2. We shall adopt a value of $\lambda = 0.2$, though it should be noted that we are less concerned here with the

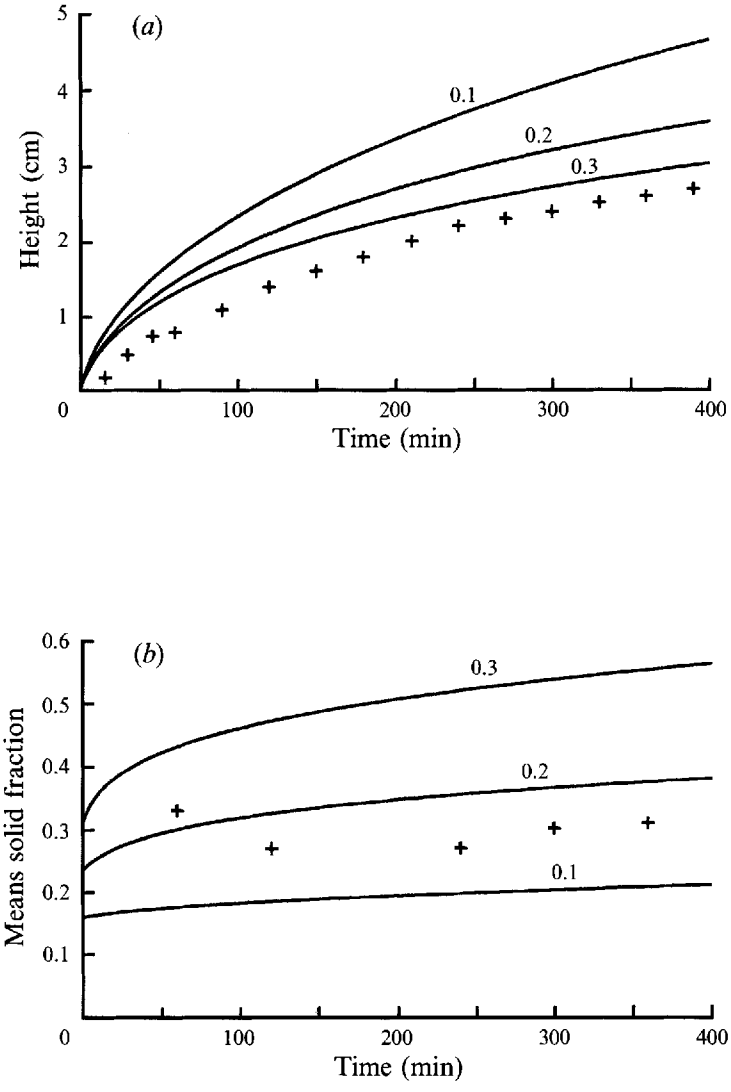

FIGURE 5. Predictions of the height of the mushy layer (*a*) and its mean solid fraction (*b*) as they evolve for three different values of the coefficient λ in the expression for solute flux (2.11) and $A = 1$. Parameter values are those for a solution of NH_4Cl contaminated with 0.5 wt% $CuSO_4$, with the kinetic coefficient calculated from (3.1). The data are from experiments by Huppert & Hallworth (1993).

accurate prediction of any particular experiment than in the variations between experiments that are contaminated to different extents by $CuSO_4$.

In figure 6(*a*), the height of the mushy layer h_i is plotted as a function of time for six different values of $\mathscr{G}$ which, according to (3.1), correspond to the different contaminations by $CuSO_4$: 0%, 0.1%, 0.2%, 0.3%, 0.5% and 1.0%. These are the levels of contamination investigated experimentally by Huppert & Hallworth (1993). Their data are plotted in figure 6(*b*) for comparison. We have shown their data only for times before chimneys were observed in their experiments, since our theory only applies while the mushy layer is stagnant. It can be seen that the theoretical calculations overpredict the measured depths of the mushy layer by up to 40%. However, the important observation for the present investigation is that the mushy layer is predicted

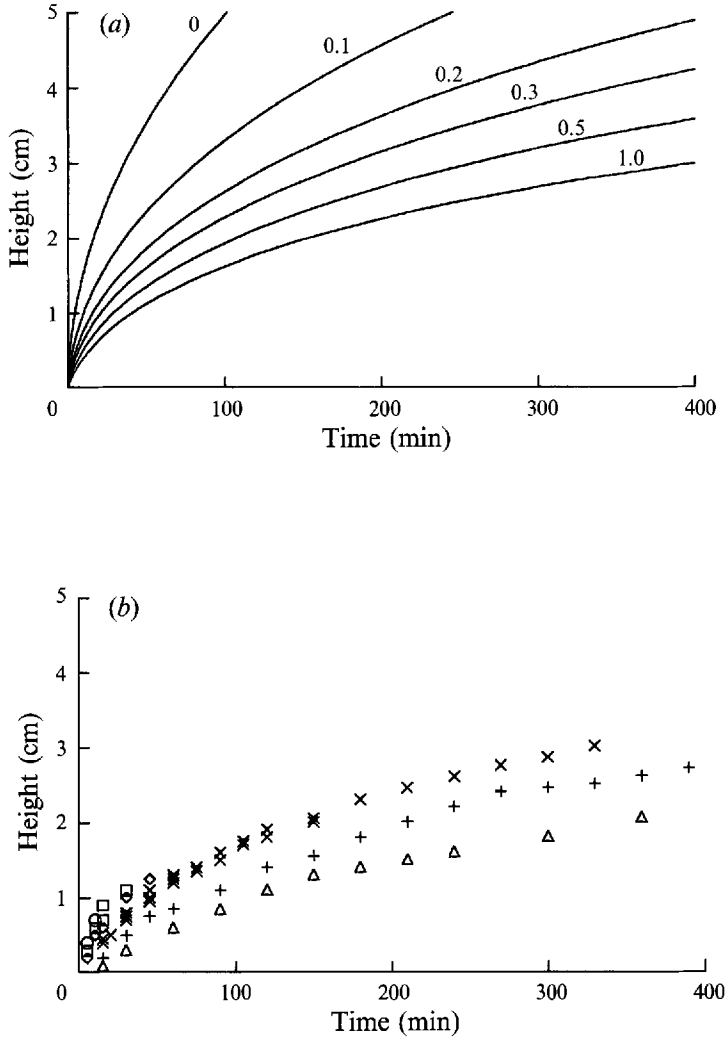

FIGURE 6. (*a*) The predicted evolutions of the height of the mushy layer for different levels of contamination. The numbers indicate the wt% $CuSO_4$ contamination. (*b*) Data from Huppert & Hallworth (1993) plotted only for times before any plumes were observed emanating from the mushy layer. Levels of contamination in the experimental data were: 0% (○); 0.1% (□); 0.2% (◇); 0.3% (×); 0.5% (+); 1.0% (△).

to grow more slowly when the level of contamination is higher, in accord with the experimental findings. Further, the fractional changes in growth rate with contamination are commensurate with those observed by Huppert & Hallworth (1993).

The slower growth is caused by two effects, which both originate from the decrease in kinetic parameter. As the contamination increases, the kinetic parameter decreases, as seen in figure 3. The interfacial undercooling is correspondingly larger for a given growth rate, which can be seen from (2.6) or from the experimental results shown in figure 3(*a*). Thus the heat flux F_T and the solute flux F_C are both increased. The increase in heat flux inhibits growth of the mushy layer directly. The increase in solute flux causes the solid fraction at the edge of the mushy layer to be larger, so that more latent heat is liberated for a given growth rate, and this too retards the rate of advance of the interface.

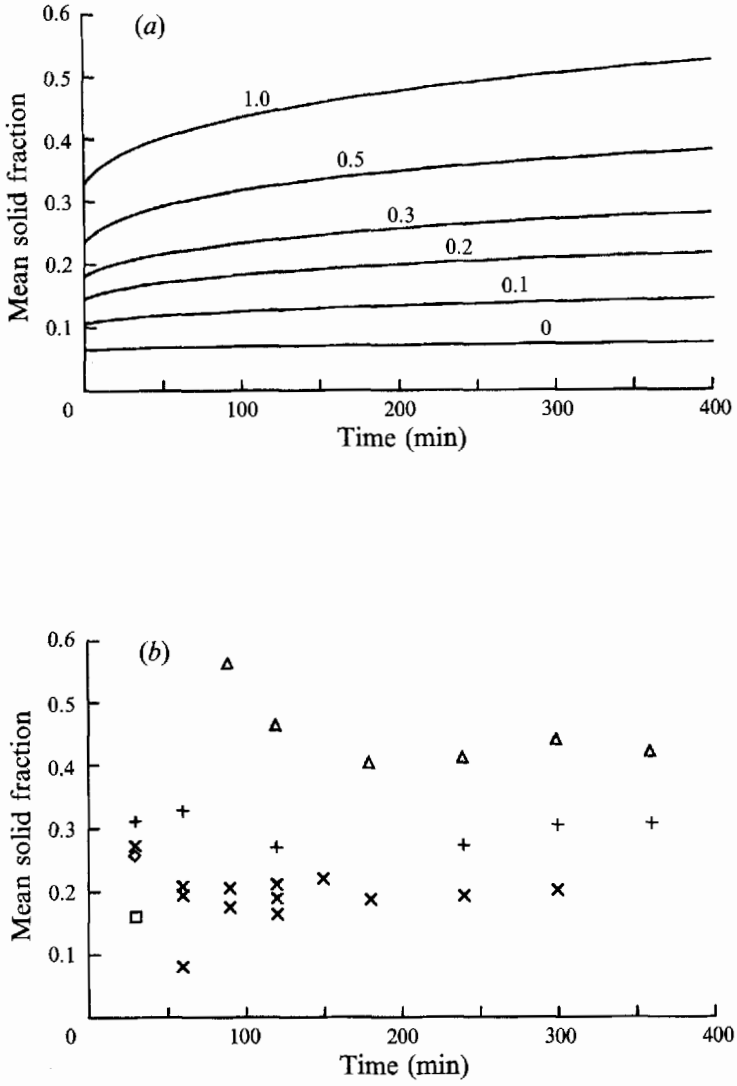

FIGURE 7. (*a*) The predicted evolutions of the mean solid fractions within the mushy layer for different levels of contamination. The numbers indicate the wt% $CuSO_4$ contamination. (*b*) Data from Huppert & Hallworth (1993) plotted only for times before any plumes were observed emanating from the mushy layer. Levels of contamination in the experimental data are indicated by the same symbols as for figure 7.

In figure 7(*a*), we see how the mean solid fraction $\bar{\phi}$ in the mushy layer increases with the contamination by $CuSO_4$. As explained above, this is a consequence of the coupled effect of interfacial disequilibrium and compositional convection. The predicted solid fractions are about 40% larger than the data of Huppert & Hallworth shown in figure 7(*b*). However, once again, the fractional change with contamination is similar in the predicted and measured results.

In figure 8(*a*), the concentration of the liquid region, which has been assumed to be well mixed, is plotted as a function of time. The concentration decreases with time owing to the convective transport of solute from the mush–liquid interface. The rate of decrease of concentration with time is predicted to increase with increased contamination. Huppert & Hallworth (1993) saw no systematic variation with

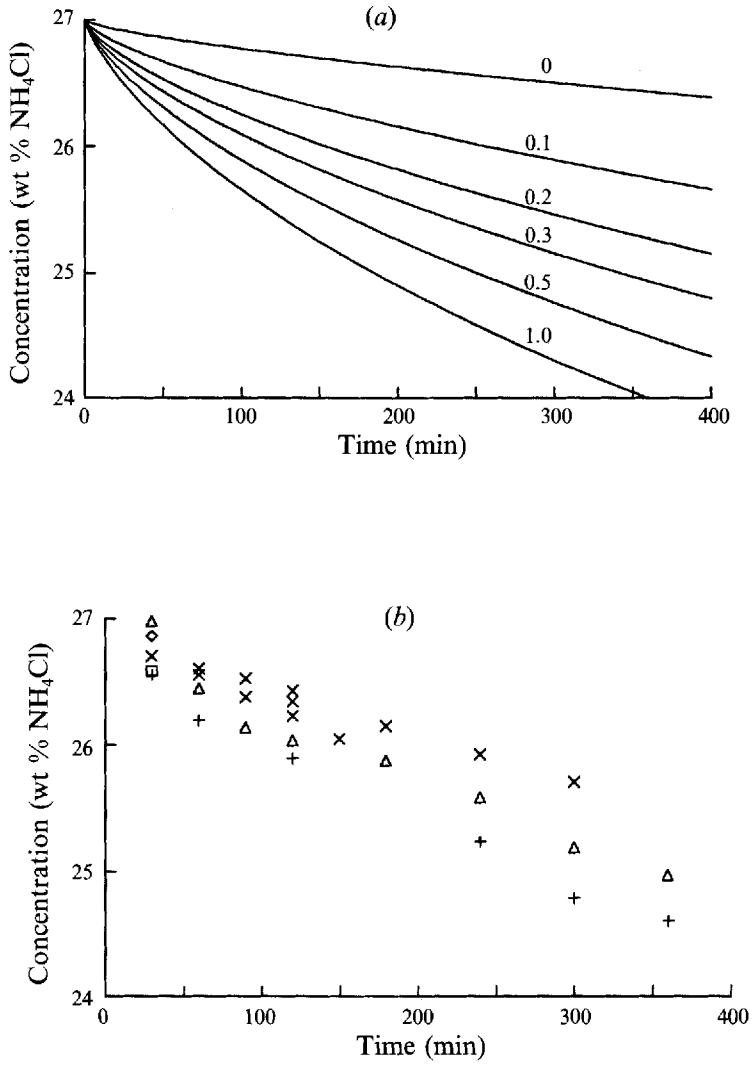

FIGURE 8. (*a*) The predicted evolutions of the concentration in the liquid region for different levels of contamination. The numbers indicate the wt% $CuSO_4$ contamination. (*b*) Data from Huppert & Hallworth (1993) plotted only for times before any plumes were observed emanating from the mushy layer. Levels of contamination in the experimental data are indicated by the same symbols as for figure 7.

contamination in their data. However, we see that if the data are restricted to times before chimneys formed (figure 8*b*), there is some indication that the rate of change of concentration increases with contamination, in line with the theoretical predictions.

5. The onset of chimney convection

One of the principal results of Huppert & Hallworth (1993) is that the onset of convection through chimneys in the mushy layer is delayed by contaminating the NH_4Cl–H_2O system with $CuSO_4$, and that chimneys are inhibited altogether once the contamination exceeds a critical value (of about 0.3 wt% in their experiments). Some explanation of this phenomenon is provided by the results of the preceding section.

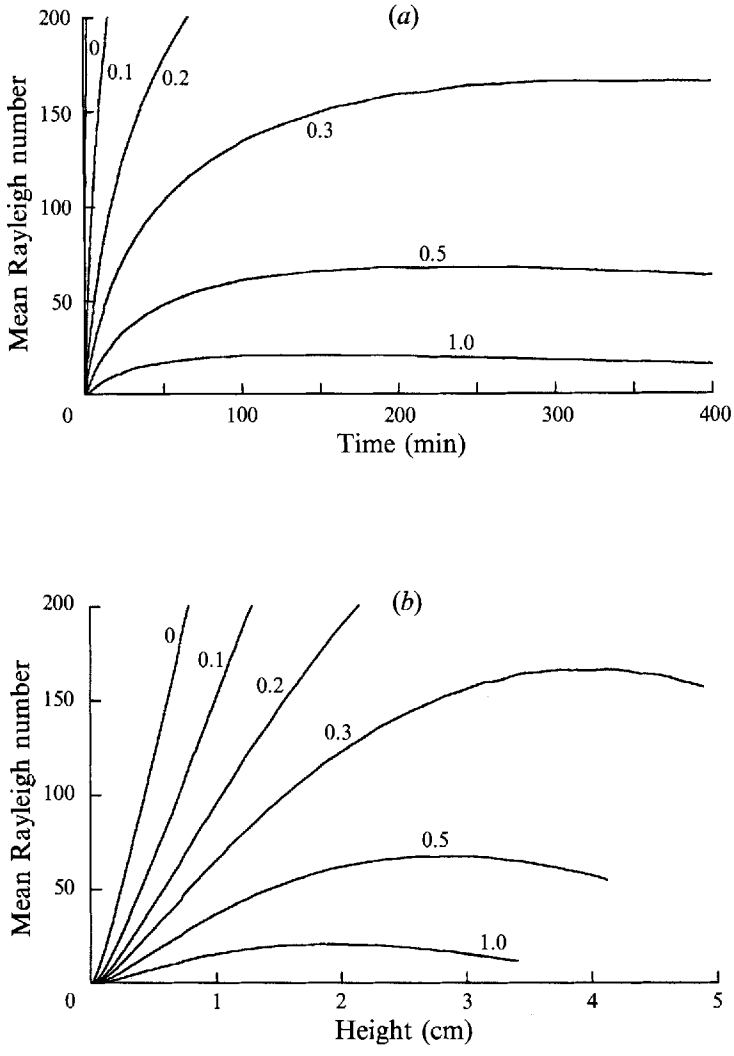

FIGURE 9. The predicted values of the mean Rayleigh number of the mushy layer as functions of time (*a*) and height of the layer (*b*) for different values of the kinetic coefficient $\mathscr{G}$ corresponding to the levels of contamination indicated by the numbers according to equation (3.1).

Worster (1992) has suggested that chimneys in mushy layers are associated with a 'mushy-layer mode' of convection, which becomes excited beyond a critical value of the Rayleigh number

$$R_m = \frac{\beta g \Delta C \Pi h_i}{\kappa \nu}, \tag{5.1}$$

where $\Delta C = C_i - C_L(T_b)$ and Π is a characteristic permeability of the mushy layer. The numerical value of the Rayleigh number depends quite strongly on the permeability, which is difficult to measure or predict. Here, we use the expression from Happel & Brenner (1986) adapted for a regular array of cylinders by Tait & Jaupart (1992) to give

$$\Pi = \tfrac{1}{8}b^2[-2\ln(1-\chi) - (1-\chi)^2 - 3 + 4(1-\chi)], \tag{5.2}$$

where $\chi = 1-\phi$ is the liquid fraction in the mushy layer and b is half the distance between primary dendrites which they estimated to be about 0.05 cm.

The predicted values of R_m from our calculations are plotted as functions of time

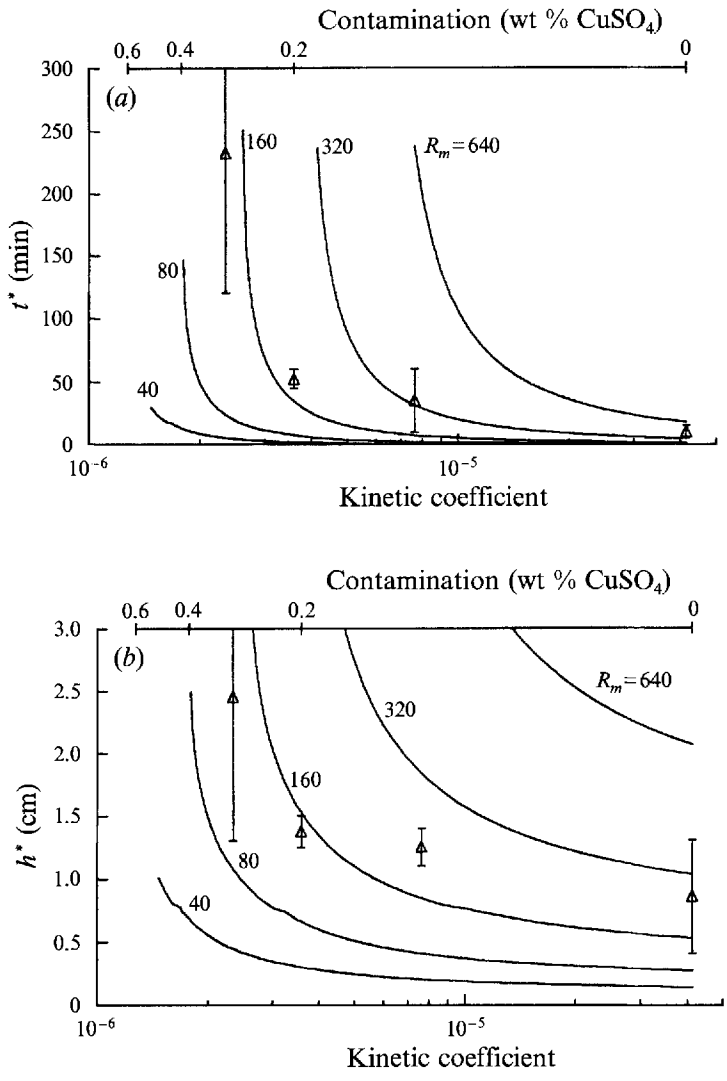

FIGURE 10. The solid lines show (*a*) the time t^* and (*b*) the height of the mushy layer h^* at which the predicted mean Rayleigh number first reaches the values indicated on the curves for a given value of the kinetic coefficient $\mathscr{G}$. The data and associated error bars indicate the times and heights at which Huppert & Hallworth (1993) first observed plumes emanating from the mushy layer. The alternative ordinate at the top of each graph is the contamination by $CuSO_4$ that gives the corresponding kinetic coefficient according to (3.1).

and of the depth of the mushy layer in figure 9*a*, *b* for six values of the coefficient $\mathscr{G}$ corresponding to the indicated levels of contamination according to (3.1). It is clear that the Rayleigh number is significantly smaller in the systems with smaller values of $\mathscr{G}$ (higher contaminations). In fact, it can be seen that the Rayleigh number first increases with time but can ultimately decrease with time as a result of the diminishing solid fraction and compositional gradient across the mushy layer. Therefore, the Rayleigh number can be bounded above, and may never reach a sufficient value to allow chimneys to form.

This is illustrated further in figure 10, where we plot, as functions of the kinetic coefficient $\mathscr{G}$, the times t^* and heights of the mushy layer h^* when the predicted Rayleigh

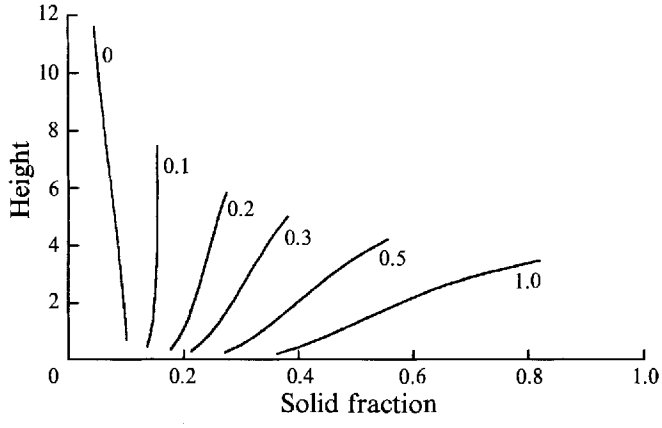

FIGURE 11. The predicted solid fraction in the mushy layer as a function of depth within the layer after 600 minutes for different values of the kinetic coefficient $\mathscr{G}$ corresponding to the levels of contamination indicated by the numbers according to equation (3.1).

number first exceeds particular values. Each curve has a vertical asymptote, which demonstrates the general result that, whatever critical Rayleigh number one might be concerned with, systems characterized by sufficiently small kinetic coefficients will never attain that Rayleigh number. Using the values of $\mathscr{G}$ that we have measured for aqueous solutions of ammonium chloride contaminated with copper sulphate (equations (3.1)), we can plot on the same graphs the observations of Huppert & Hallworth (1993) of the first sightings of chimneys. These data follow similar trends to the theoretical curves, which suggests that the delay in formation of chimneys is related to the time taken for the Rayleigh number of the mushy layer to attain some critical value. This value appears to be much larger than the critical values (of order 10) predicted for linear instability of mushy layers (Worster 1992), though one must beware of determining critical values from such transient experiments. It is to be expected, however, that chimneys will appear only some time after the critical conditions for convection have been reached, since the formation of chimneys requires convection of finite amplitude.

A further consequence of the model presented in this paper is illustrated in figure 11. Here we plot the solid fraction in the mushy layer as a function of height after an elapsed time of 600 minutes. The solid fraction is dependent on height and the figure shows that use of the mean solid fraction in the estimation of the permeability may be a rather gross approximation. In particular, it is seen that the solid fraction can increase upwards (especially at large contaminations) which will put a 'lid' on the mushy layer and inhibit convection further. Note that, unlike the other results in this paper, this latter qualitative effect is sensitive to the form of the kinetic equation (2.6). For example, the solid fraction would always be predicted to decrease upwards if the kinetic law were linear rather than quadratic.

6. Discussion

A model has been formulated for the growth of a mushy layer cooled from below that incorporates important interactions between interfacial undercooling and compositional convection within the melt. The degree of undercooling was measured during the solidification of ammonium chloride from its aqueous solution contaminated to various degrees by copper sulphate. Small levels of contamination were

found to have a very strong effect on the interfacial undercooling. These findings were used in numerical evaluations of the theoretical model to predict how the evolution of a stagnant mushy layer is affected by compositional convection in the melt for different levels of contamination.

It is found that when the kinetic parameter is smaller (when the contamination is greater) the height of the mushy layer grows more slowly, the solid fraction within the mushy layer is larger, and the composition of the melt evolves more rapidly. These effects all conspire to make the Rayleigh number associated with the mushy layer evolve more slowly and, though it always increases at first, the Rayleigh number can ultimately decrease with time. Therefore, the time at which any particular (critical) value of the Rayleigh number is reached is increased by the contamination. Indeed, the Rayleigh number may never reach its critical value in systems with sufficiently slow kinetics. Under the hypothesis that chimneys within mushy layers are generated by convection within the mushy layer that is initiated at some critical value of the Rayleigh number, this analysis shows that the time at which chimneys first appear will be longer in systems that have greater levels of interfacial undercooling. And some systems may solidify completely without ever producing chimneys.

These findings are consistent with the experimental results of Huppert & Hallworth (1993). In particular, it has been shown that the effects of compositional convection coupled with interfacial undercooling are of sufficient magnitude to explain the huge variations discovered by Huppert & Hallworth when aqueous solutions of ammonium chloride are tainted with small amounts of copper sulphate. The measured times for chimneys to appear are commensurate with the predicted times for the Rayleigh number of the mushy layer to reach a value of order 10^2.

The analysis of the present paper may also explain the apparent discrepancy in the findings of Tait & Jaupart (1992) and Tait, Jahrling & Jaupart (1992), who found the critical Rayleigh number for onset of convection to be about 20 or about 80 respectively. These authors estimated the Rayleigh number of the mushy layer by assuming that its solid fraction was equal to the value it would have during diffusion-controlled growth (Worster 1986). We have seen here that the solid fraction in the mushy layer is increased by the compositional convection above it. Tait *et al.* (1992) cooled the base of their experimental tank more slowly than did Tait & Jaupart (1992). This would have allowed the transient effects described in this paper more time to act and would, in particular, have caused the solid fraction to have been larger than estimated. The actual value of the Rayleigh number at onset of convection would therefore have been lower than the value, 80, that they estimated.

The model that has been analysed in this paper has provided quantitive evidence and support for the idea that the level of interfacial undercooling (which depends in large part on the chemistry of the system being analysed) is a key parameter determining the onset of chimney-forming convection in mushy layers cooled from below. However, a number of approximations were made in the development of the model that need to be borne in mind when interpreting its predictions.

In the basic model described in §2, any contraction or expansion due to the difference in density between the solid and liquid phases has been ignored. This may lead to errors of about 20% in the prediction of the height and solid fraction of the mushy layer in the case of ammonium chloride being crystallized from its aqueous solution.

The use of a mean Rayleigh number to determine the onset of convection in the mushy layer is rather crude since the solid fraction (and hence permeability) of the mushy layer can vary significantly with its depth (Worster 1991; Tait *et al.* 1992).

Worster (1992) has shown that the distribution of solid fraction within the mushy layer has a large effect on the critical Rayleigh number for the mushy-layer mode of convection.

We have assumed throughout that the permeability of the mushy layer depends only on its porosity. However, systems with slower kinetics are also characterized by having less branched crystals and will therefore produce mushy layers of greater permeability for the same porosity and primary crystal spacing. This may counter somewhat the effects on the Rayleigh number discussed in this paper.

Finally, it has been assumed that the interior of the mushy layer is in local thermodynamic equilibrium, even though the interfacial region is significantly undercooled. It is an important objective of future research to determine experimentally whether the interior of the mushy layer is undercooled and to model the effects of internal undercooling theoretically, if it is found to be significant. As suggested by S. Lipson in an appendix to Huppert & Hallworth (1993), such internal undercooling may inhibit the formation of chimneys further, even once the interstitial fluid of the mushy layer is convecting.

The present model predicts that the solid fraction in the mushy layer can increase away from the cold boundary in systems characterized by large interfacial undercooling, as a consequence of the compositional convection in the melt. This phenomenon, which is not predicted by equilibrium theories of mushy layers, may be important in the formation of sea ice, for example. The same physical processes also result in macrosegregation of the solidifying system and may be an important mechanism causing zonation in magma chambers and segregation in industrial castings.

7. Addendum

We also attempted to measure the variation of the kinetic coefficient associated with the growth of a mushy layer from aqueous solutions of ammonium bromide contaminated with small amounts of copper sulphate. Huppert & Hallworth (1993) had found no inhibition of chimneys in this system with contamination up to 1 wt%.

There is a much greater degree of uncertainty surrounding the experiments with the ammonium-bromide system owing to the formation of hydrated copper (II) bromide complexes in solution (Huppert & Hallworth 1993). These render the solution increasingly opaque as the concentration of $CuSO_4$ increases, which makes visual observations of chimneys and of the position of the interface difficult. Our results for this system are therefore limited. They are illustrated in figure 12, and can be summarized as follows.

The first point to notice is that the kinetic coefficient determined for the uncontaminated NH_4Br solutions (5.0×10^{-5} cm s^{-1} °C^{-2}) is similar in magnitude to, but a little larger than, that found for uncontaminated NH_4Cl solutions (4.1×10^{-5} cm s^{-1} °C^{-2}). The slower growth rates of NH_4Br mushy layers found by Huppert & Hallworth (1993) (their figure 10) is almost certainly due to the fact that the parameter $\mathscr{C} = (C_s - C_L(T_B))/(C_0 - C_L(T_B))$ was smaller in their experiments with NH_4Br, which would cause the solid fraction to have been larger (Worster 1991; and see Huppert & Hallworth 1993, figure 12*a*) and would therefore mean that the latent heat released per unit increase in height of the mushy layer would have been larger.

Next we would point out that adding $CuSO_4$ to the NH_4Br solutions does not reduce the kinetic coefficient nearly as much as when similar quantities of $CuSO_4$ are added to NH_4Cl solutions. In particular, the kinetic coefficient for NH_4Br contaminated with

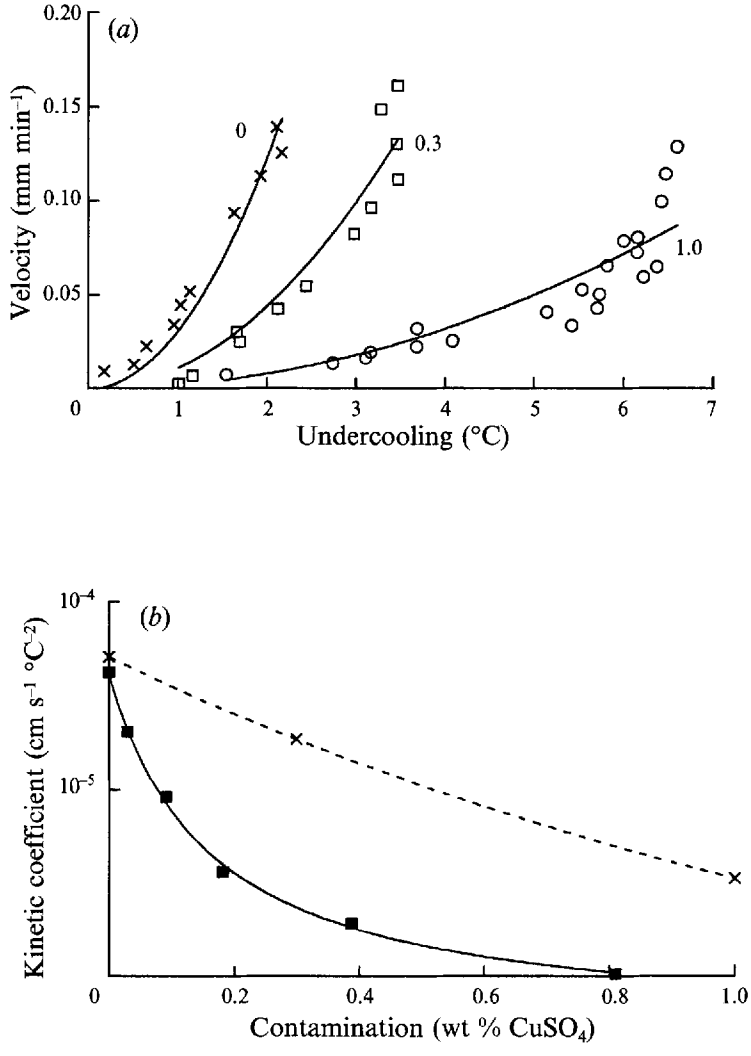

FIGURE 12. (*a*) Experimental data of the rate of growth of mushy layers of NH_4Br crystals grown from aqueous solutions contaminated to varying degrees with $CuSO_4$, as functions of the interfacial undercooling. The results of several different experiments are shown. Results from experiments that used the same level of contamination (indicated in wt% $CuSO_4$ by the numbers on the graph) are plotted using the same symbol. The solid curves represent the best-fit second-order power law for each set of data for the same level of contamination. (*b*) The crosses show the coefficients of the power laws found from (*a*) plotted as a function of the level of contamination. The dashed curve is a smooth interpolation of the data. Also shown, for comparison, are the data from figure 3(*b*) for the NH_4Cl system.

1 wt% $CuSO_4$ is approximately 3.3×10^{-6} cm s^{-1} °C^{-2}, which is more than twice as large as the kinetic coefficient (approximately 1.5×10^{-6} cm s^{-1} °C^{-2}) for NH_4Cl contaminated with just 0.5 wt% $CuSO_4$, which is the level of contamination at which chimneys were not apparent in the experiments of Huppert & Hallworth (1993). Although many other parameters enter into the determination of the Rayleigh number of the mushy layer, this result, together with the model proposed herein, seems consistent with the observation of Huppert & Hallworth (1993) that up to 1 wt% $CuSO_4$ did not affect the occurrence of chimneys in the NH_4Br mushy layers. There is,

however, some decrease in kinetic coefficient with contamination, which suggests that a sufficient quantity of $CuSO_4$ may prevent the formation of chimneys in the NH_4Br system. At higher concentrations, however, the contamination should perhaps not be treated as small and a full treatment of three-component solidification should be sought.

We are indebted to M. A. Hallworth and H. E. Huppert for providing us with data from their experiments. We are also very grateful to them and to J. S. Wettlaufer and A. W. Woods for useful discussions about this work and for reviewing earlier drafts of the manuscript. The work of M.G.W. is supported by NERC and by the National Aeronautics Space Administration through the Microgravity Science and Applications Division. R.C.K. gratefully acknowledges a travel grant from the British Council.

REFERENCES

CHEN, C. F. & CHEN, F. 1991 Experimental study of directional solidification of aqueous ammonium chloride solution. *J. Fluid Mech.* **277**, 567–586.

CHIARELI, A. O. P., HUPPERT, H. E. & WORSTER, M. G. 1994 Segregation and flow during the solidification of alloys. *J. Cryst. Growth* (in press).

COPLEY, S. M., GIAMEI, A. F., JOHNSON, S. M. & HORNBECKER, M. F. 1970 The origin of freckles in binary alloys. *IMA J. Appl. Maths* **35**, 159–174.

EMMS, P. W. & FOWLER, A. C. 1994 Compositional convection and freckle formation in the solidification of binary alloys. *J. Fluid Mech.* **262**, 111–139.

FLOOD, S. C. & HUNT, J. D. 1987 A model of a casting. *Appl. Sci. Res.* **44**, 27–42.

HAPPEL, J. & BRENNER, H. 1986 *Low Reynolds Number Hydrodynamics*, p. 533. M. Nijhoff.

HILLS, R. N. & ROBERTS, P. H. 1993 A note on the kinetic conditions at a supercooled interface. *Intl Commun. Heat Mass Transfer* **20**, 407–416.

HOWARD, L. N. 1966 Convection at high Rayleigh number. In *Proc. 11th Intl Congr. Appl. Mech., Munich*, pp. 1109–1115. Springer.

HUPPERT, H. E. 1990 The fluid dynamics of solidification. *J. Fluid Mech.* **212**, 209–240.

HUPPERT, H. E. & HALLWORTH, M. A. 1993 Solidification of NH_4Cl and NH_4Br from aqueous solutions contaminated by $CuSO_4$: the extinction of chimneys. *J. Cryst. Growth* **130**, 495–506.

KERR, R. C., WOODS, A. W., WORSTER, M. G. & HUPPERT, H. E. 1990*a* Solidification of an alloy cooled from above. Part 1. Equilibrium growth. *J. Fluid Mech.* **216**, 323–342.

KERR, R. C., WOODS, A. W., WORSTER, M. G. & HUPPERT, H. E. 1990*b* Solidification of an alloy cooled from above. Part 2. Non-equilibrium interfacial kinetics. *J. Fluid Mech.* **217**, 331–348.

KIRKPATRICK, R. J., ROBINSON, G. R. & HAYS, J. F. 1976 Kinetics of crystal growth from silicate melts: anorthite and diopside. *J. Geophys. Res.* **81**, 5715–5720.

TAIT, S., JAHRLING, K. & JAUPART, C. 1992 The planform of compositional convection and chimney formation in a mushy layer. *Nature* **359**, 406–408.

TAIT, S. & JAUPART, C. 1989 Compositional convection in viscous melts. *Nature* **338**, 571–574.

TAIT, S. & JAUPART, C. 1992 Compositional convection in a reactive crystalline mush and melt differentiation. *J. Geophys. Res.* **97**(B5), 6735–6756.

TURNER, J. S. 1979 *Buoyancy Effects in Fluids*. Cambridge University Press.

TURNER, J. S., HUPPERT, H. E. & SPARKS, R. S. J. 1986 Komatiites II: Experimental and theoretical investigations of post-emplacement cooling and crystallization. *J. Petrol.* **27**, 397–437.

WOODS, A. W. & HUPPERT, H. E. 1989 The growth of compositionally stratified solid by cooling a binary alloy from below. *J. Fluid Mech.* **199**, 29–55.

WORSTER, M. G. 1986 Solidification of an alloy from a cooled boundary. *J. Fluid Mech.* **167**, 481–501.

WORSTER, M. G. 1991 Natural convection in a mushy layer. *J. Fluid Mech.* **224**, 335–359.

WORSTER, M. G. 1992 Instabilities of the liquid and mushy regions during solidification of alloys. *J. Fluid Mech.* **237**, 649–669.

WORSTER, M. G., HUPPERT, H. E. & SPARKS, R. S. J. 1990 Convection and crystallization in magma cooled from above. *Earth Planet. Sci. Lett.* **101**, 78–89.

WORSTER, M. G., HUPPERT, H. E. & SPARKS, R. S. J. 1993 The crystallization of lava lakes. *J. Geophys. Res.* **98**, 15891–15901.